Supplemental data are available at www.sciencemag.org/feature/data/1052815.shl.
22. ε^{92}Zr values of the Ti-rich minerals are systematically lower by ~1 ε unit, although the values are still within the analytical error of the AMES value. This feature is caused by (i) Ti in the Zr fraction (Ti/Zr ratio of ~1 to 5 for Ti minerals) and (ii) the ^{93}Nb tail on the baseline of ^{92}Zr. Because Nb was separated together with Zr from the whole rock matrix, this element may cause problems during ^{92}Zr measurements if Nb/Zr > 1. Such high Nb/Zr ratios were not present in the solutions of other samples.
23. Terrestrial ε^{92}Zr in two 1.2-Ga allanite and pitchblende samples from India, which have high U-Th contents, rules out any substantial ^{92}Zr contribution from secondary, post-Hadean spallation processes. U-Th–induced α-particle irradiation of Nb, Mo, or Y can produce ^{92}Nb and thus ^{92}Zr [(*14*); K. E. Apt, J. D. Knight, D. C. Kamp, R. W. Perkins, *Geochim. Cosmochim. Acta* **38**, 1485 (1974)].
24. P. D. Kinney, *Earth Planet. Sci. Lett.* **79**, 337 (1986).
25. A. Kröner, W. Compston, I. S. Williams, *Tectonophysics* **161**, 271 (1989).
26. R. Maas and M. T. McCulloch, *Geochim. Cosmochim. Acta* **55**, 1925 (1991).
27. P. D. Kinney and A. P. Nutman, *Precambrian. Res.* **78**, 165 (1996).
28. M. Lopez-Martinez, D. York, J. A. Hanes, *Precambrian. Res.* **57**, 91 (1992).
29. M. Tredoux, R. J. Hart, R. W. Carlson, S. B. Shirey, *Geology* **27**, 923 (1999).
30. Impact spherules of the lower Fig Tree Group, of which ~50% were supplied from a chondritic impactor, have ^{53}Cr/^{52}Cr values lower than the bulk Earth value, typical of carbonaceous chondrites [A. Shukolyukov, F. T. Kyte, G. W. Lugmair, D. R. Lowe, G. R. Byerly, in *Impacts and the Early Earth*, I. Gilmour and C. Koeberl, Eds. (Springer, Heidelberg, Germany, 2000), vol. 92, pp. 99–116.].
31. The CAI-free Allende sample is a handpicked separate from which visible CAIs were separated. Adrar 003 is an extraordinarily unequilibrated primitive type 3 ordinary chondrite [A. Bischoff, D. W. G. Sears, P. H. Benoit, T. Geiger, T. Stöffler, *LPSCI Contrib.* **XXIII**, 107 (1992)]. A ^{92}Zr anomaly in a 60-mg split of Adrar 003 confirms that heterogeneities in Zr/Nb are preserved on a mineral but not on a bulk rock scale. Sahara 97096 is a primitive enstatite chondrite [L. Grossman, *Meteorit. Planet. Sci.* **33**, A221 (1998)].
32. The Allende CAI A-37 has been described in detailed by A. Bischoff and H. Palme [*Geochim. Cosmochim. Acta* **51**, 2733 (1987)] and by A. Bischoff, H. Palme, and B. Spettel [*LPSCI Contrib.* **XVIII**, 81 (1987)].
33. C. Göpel, G. Manhès, C. J. Allègre, *Meteoritics* **26**, 338 (1991).
34. A. S. Kornacki and B. Fegley Jr., *Earth Planet. Sci. Lett.* **79**, 217 (1986).
35. B. Stewart, D. A. Papanastassiou, G. J. Wasserburg, *Earth Planet. Sci. Lett.* **143**, 1 (1996).
36. H. Takeda, D. D. Bogard, D. W. Mittlefehldt, D. H. Garrison, *Geochim. Cosmochim. Acta* **64**, 1311 (2000).
37. Dar al Gani 262 and 400 are anorthositic lunar highland breccias [A. Bischoff *et al.*, *Meteorit. Planet. Sci.* **33**, 1243 (1998); J. Zipfel *et al.*, *Meteorit. Planet. Sci.* **33**, A171 (1998)].
38. S. R. Taylor and S. M. McLennan, *Rev. Geophys.* **33**, 241 (1995), and references therein.
39. S. J. G. Galer and S. L. Goldstein, *Geochim. Cosmochim. Acta* **55**, 227 (1991).
40. R. W. Carlson and G. W. Lugmair, *Earth Planet. Sci. Lett.* **90**, 119 (1988).
41. G. A. Snyder, L. A. Taylor, C. R. Neal, *Geochim. Cosmochim. Acta* **56**, 3809 (1992), and references therein.
42. J. Li and C. B. Agee, *Nature* **381**, 686 (1996).
43. Assuming partition coefficient $D_{liq/melt}$ of 9 for Zr and 0.1 to 1 for Nb in Mg-perovskite (*12*), equilibrium crystallization and the subsequent separation of 1% perovskite from Earth's primitive mantle [~10 parts per million (ppm) of Zr and 0.6 ppm of Nb] results in a reservoir that has ~80 ppm of Zr and Zr/Nb > 100. Therefore, a Mg-perovskite reservoir would have extremely low ε^{92}Zr (less than −1) if it had formed within the first 50 My after formation of the solar system (Fig. 2A). The addition of ~10% of this reservoir to a younger depleted mantle (ε^{92}Zr = 0, ~6 ppm of Zr) could have generated ε^{92}Zr values that are lower than the silicate Earth value.
44. S. L. Goldstein, R. K. O'Nions, P. J. Hamilton, *Earth Planet. Sci. Lett.* **70**, 221 (1984).
45. This work was supported by grants Me 1717/1-1 and ZG 3/16 of the German Research Council (Deutsche Forschungsgemeinschaft). We thank C. Ballhaus, G. Hanson, E. Scherer, and H. Palme for fruitful discussions. F. Tomaschek, E. Krogstad, K. Rickers, A. Kröner, E. Trapp, M. Bröcker, R. Schumacher, J. Zipfel, and the Barberton Branch of the Geological Society of South Africa generously provided samples or helped during sampling campaigns. Journal reviews by four anonymous referees are appreciated.

9 March 2000; accepted 17 July 2000

A 22,000-Year Record of Monsoonal Precipitation from Northern Chile's Atacama Desert

J. L. Betancourt,[1]* C. Latorre,[2] J. A. Rech,[3] J. Quade,[3] K. A. Rylander[1]

Fossil rodent middens and wetland deposits from the central Atacama Desert (22° to 24°S) indicate increasing summer precipitation, grass cover, and groundwater levels from 16.2 to 10.5 calendar kiloyears before present (ky B.P.). Higher elevation shrubs and summer-flowering grasses expanded downslope across what is now the edge of Absolute Desert, a broad expanse now largely devoid of rainfall and vegetation. Paradoxically, this pluvial period coincided with the summer insolation minimum and reduced adiabatic heating over the central Andes. Summer precipitation over the central Andes and central Atacama may depend on remote teleconnections between seasonal insolation forcing in both hemispheres, the Asian monsoon, and Pacific sea surface temperature gradients. A less pronounced episode of higher groundwater levels in the central Atacama from 8 to 3 ky B.P. conflicts with an extreme lowstand of Lake Titicaca, indicating either different climatic forcing or different response times and sensitivities to climatic change.

The tropics are believed to be an important source of global climate variability at various time scales, yet their role is poorly understood. Ice age cooling (~5°C) of the tropics is now evident from many tropical ocean and land records (*1*), raising questions about climate forcing by high versus low latitudes. Precise chronologies of tropical climate change are becoming increasingly necessary to place empirical constraints on competing theories and models. Here, we focus on monsoonal circulation and tropical rainfall over the central Andes. One measure of monsoonal circulation over the central Andes is the variability of summer precipitation (December to March) that spills over from the Altiplano to the Atacama Desert, representing the abrupt, tail end of the tropical rainfall belt.

A history of vegetation change and groundwater fluctuations was reconstructed from ^{14}C dated fossil rodent middens (*2*) and wetland deposits (*3*) at sites straddling the Tropic of Capricorn (23.5°N) in the central Atacama Desert (Figs. 1 and 2). In the Atacama, several rodents (*Lagidium*, *Phyllotis*, *Abrocoma*, and *Octodontomys*) make urine-hardened cave deposits rich in plant remains akin to North American packrat middens (*2*). Rodent middens afford high taxonomic, spatial, and temporal resolution of past vegetation growing on dry hillslopes and in this study provide important evidence for seasonality of rainfall. Midden records, however, are stratigraphically discontinuous and represent only snapshots of flora through time. In contrast, paleosprings, fed by precipitation in the Andes (>3500 m), have left behind diatomaceous wetland deposits (*3*) that provide a more continuous record of sustained hydrologic changes in the Atacama Desert. The two data sets are strongly complementary and together provide a record of paleoclimatic change that is unprecedented for the region.

Most of the annual precipitation in the Calama and Salar de Atacama basins (Fig. 2) falls in summer but shifts to winter (June to September) only 200 km to the south (Fig. 1). This sharp gradient in seasonality is reflected in southern limits of ~22° to 24°S for most plants that flower in summer versus northern limits of ~25° to 27°S for those that flower in winter (*4*).

[1]U.S. Geological Survey, 1675 West Anklam Road, Tucson, AZ 85745, USA. [2]Laboratorio de Botanica, Facultad de Ciencias, Universidad de Chile, Casilla 653, Santiago, Chile. [3]Department of Geosciences, University of Arizona, Tucson, AZ 85721, USA.

*To whom correspondence should be addressed. E-mail: jlbetanc@usgs.gov

Vegetation zonation in the study area parallels orographic effects. The 0°C mean annual isotherm marks the upper limit of vascular plants at ~4500 m. Between 3800 and 4500 m, mean annual precipitation of 150 to 230 mm supports Andean steppe grasses (*Festuca ortophylla*, *Jarava frigida*, *Stipa chrysophylla*, and *Deyeuxia* spp.) and cushion plants (*Azorella compacta*). Between 3200 and 3800 m, precipitation of 70 to 150 mm supports Tolar shrubs (*Parastrephia* spp., *Chuquiraga* spp., *Lampaya medicinalis*, *Junellia seriphioides*, and *Fabiana* spp.), columnar cacti (*Trichocereus atacamensis* and *Oreocereus leucotrichus*), and summer annuals (Poaceae and Asteraceae). Salt-tolerant shrubs (*Atriplex imbricata*), cushion cacti (*Opuntia camachoi*), and a few annuals (Boraginaceae, Malvaceae, Portulacaceae, and Solanaceae) characterize the Prepuna from 2600 to 3200 m, where mean annual temperature is ~10°C and annual precipitation ranges from 20 to 70 mm. The Prepuna gives way to the Absolute Desert, a vast, barren landscape that lacks vegetation because of years or decades without any rain.

Plant macrofossils were identified from 49 dated middens between 3200 and 2400 m. Most of the middens come from Lomas de Tilocalar and Lomas de Quilvar at the southeastern end of Salar de Atacama (Fig. 2). Modern plant cover within 100 m of the middens, roughly the foraging range of the rodents, is <1% and is produced by <five species. The total number of taxa identified across all middens was 41, and individual middens contained from 6 to 25 taxa. We focused on grass point occurrence (*5*) in fossil middens because local grasses are excellent indicators of both the amount and seasonality of past rainfall (Fig. 3); more importantly, grasses do not presently grow near any of our sites.

The lack of middens from some intervals, such as 35 to 22 ky B.P., may reflect aridity and decreased midden production rather than simple decay of older middens. Four middens, found under well-exposed ignimbrite boulders, dated >40 ky B.P., suggest that degradation of older middens is not a major issue. We cannot totally rule out preservation factors, however, so we limit our inferences to the past 22 ky B.P. The oldest midden with a finite date (22 ky B.P.) has low taxonomic richness and grass abundance (Fig. 3), compared with middens dated at 16.2, 13.2, and 12.5 ky B.P. Clustering of 15 middens between 11.8 and 10.5 ky B.P., with rich floras dominated by grasses (average point occurrence of 58%) and higher elevation shrubs, indicates that this was the wettest period of the past 22 ky. Midden floras between 16.2 and 10.5 ky B.P. contain perennial C_3 steppe grasses (*Stipa chrysophylla*, *Nasella arcuata*, and *Anatherostipa venusta*), summer-flowering C_4 perennial grasses (*Enneapogon desvauxii* and *Pappophorum* sp.), C_4 annual grasses (*Munroa decumbens*, *Aristida adscensionis*, and *Chondrosum simplex*), summer annual herbs (*Schkuhria multiflora* and *Tagetes multiflora*), and Tolar shrubs (*Junellia seriphoides*, *Adesmia* sp., and *Krameria lappaceae*) and cacti (*Trichocereus* sp.) that no longer occur at the midden sites. *Nasella arcuata* is now rare in the central Atacama but common above 3800 m on the Bolivian Altiplano and in the Andes near the Peru-Chile border. *Trichocereus* sp. and all of the C_4 grasses and summer annuals today reach their southernmost limit within 50 km of the midden sites. *Pappophorum* sp., a common grass in southern Peru and northwestern Argentina, no longer occurs in northern Chile.

Grass point occurrence drops below 5%,

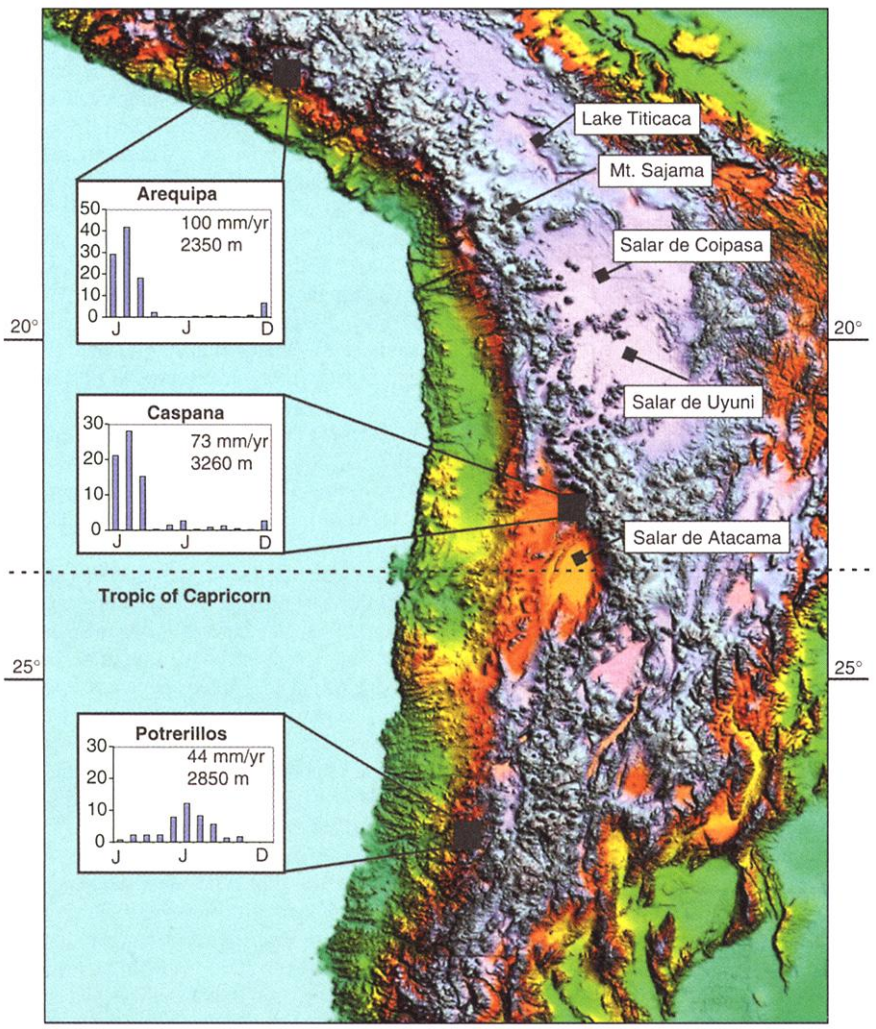

Fig. 1. Digital Elevation Map (DEM) of the subtropical Andes showing precipitation seasonality in the Atacama Desert and key sites. Approximate elevations are >4000 m (blue), 4000 to 3500 m (pink), 3500 to 3000 m, 3500 to 2500 m (brown), 2500 to 1000 (yellow), and <1000 m (green). Broad areas of pink denote the Bolivian/Peruvian Altiplano. The steep north-south gradient in rainfall seasonality between 24° and 26°S is attributable to the extreme rain shadow imposed on the easterly trades by the Chilean Andes in summer and the equally abrupt blocking of the southern westerlies by the South Pacific Anticyclone in winter.

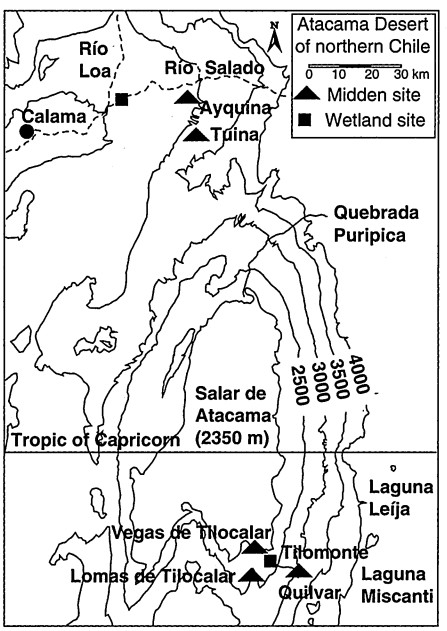

Fig. 2. Location of rodent middens and wetland deposits in the Calama and Salar de Atacama basins.

and the total number of Tolar taxa declines sharply after 10.5 ky B.P. This pattern persists until after 7.1 ky, when Tolar taxa (*Trichocereus* sp., *Krameria lappacea*, and *Junellia seriphoides*) reappear. Mid-Holocene middens resemble modern assemblages but are punctuated by more taxa, occasional appearances of Tolar taxa, and C_4 grasses (most notably *Aristida adscensionis* and *Pappophorum* sp.), with noticeable increases in grass point occurrence at 6.2, 5.1, 4.8, and 3.9 ky B.P. Ten middens from 6.2 to 3.9 ky average ~7% grass, whereas the remaining eleven middens postdating 3.0 ky B.P. average <2%.

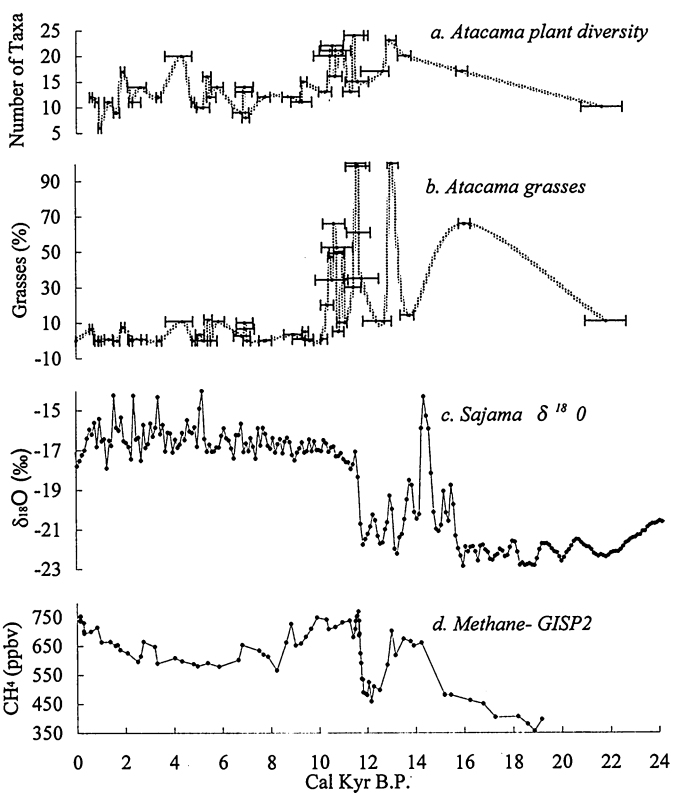

Fig. 3. Time series of (**A**) taxonomic richness (total number of all plant taxa) and (**B**) grass point occurrence (%) in rodent middens from the central Atacama Desert. Symbols are calibrated radiocarbon ages (calendar ky B.P.) with horizontal error bars representing the range of ages at 1σ. Also shown are (**C**) $\delta^{18}O$ from the Sajama ice core (*14*) and (**D**) CH_4 concentrations from the Greenland Ice Sheet Project 2 (GISP2) ice core in Greenland, which are thought to reflect changes in the extent of tropical wetlands worldwide (*24*).

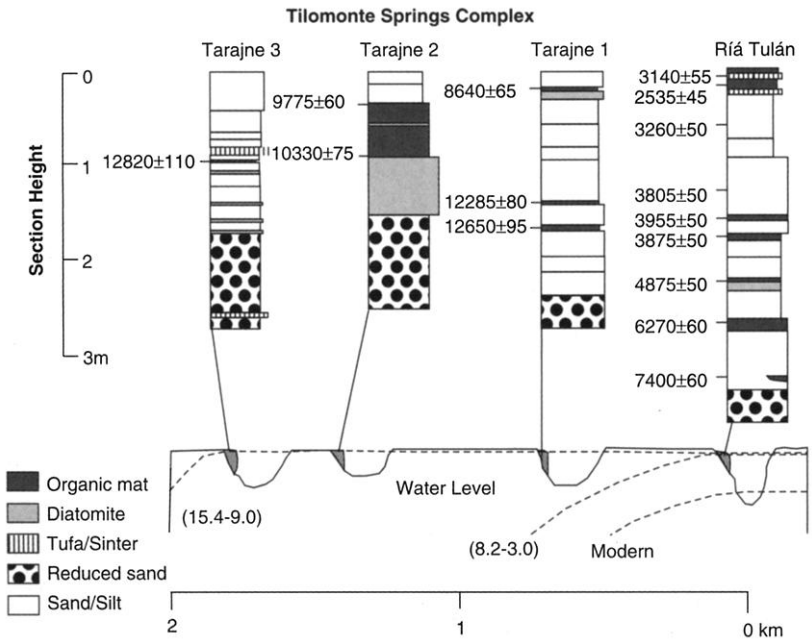

Fig. 4. Schematic of stratigraphic relations and ages (^{14}C years) of wetland deposits and relative water-table heights at the Tilomonte springs complex. Dashed lines indicate reconstructed water levels.

Paleowetland deposits at Tilomonte provide comparable evidence of hydrological changes. Tilomonte encompasses two adjacent spring complexes (Tarajne and Río Tulán) at the base of the Andes between 2500 and 2700 m, <10 km from the Lomas de Tilocalar and Lomas de Quilvar midden sites. Spring-related sediments are composed of fluvial sands and gravels, interbedded with organic-rich diatomites, tufas, and silt deposited in wetlands. Radiocarbon dates on carbonized wood, organic matter encased within tufas, and residual and humate fractions of organic mats provide a chronology of water-level fluctuations free from hard-water effects (*6*). Paleowetland deposits at Tarajne are higher above the current water table than those at Rio Tulán. The Tarajne deposits date between 15.4 and 9.0 ky B.P. (Fig. 4), thus recording when groundwater levels were highest during the late glacial–early Holocene. After 9.0 ky B.P., the water table dropped to near modern levels. Between 8.2 and 3.0 ky B.P., paleowetland deposits within Río Tulán record a less pronounced water table rise of ~11 m above the current levels (Fig. 4). Eleven meters of incision by Rio Tulán accompanied a second water table drop between 3.0 and 0.8 ky B.P.

Synchroneity between Tilomonte and three wetland records argues for shared paleohydrologic controls and rapid responses to climate changes in their collective recharge area, the Chilean Andes. Lake levels on the southern Altiplano just to the east of Salar de Atacama display changes (*7, 8*) synchronous with wetlands at El Tarajne. Lakes rose between 15.5 and 14.0 ky B.P., peaked between 12.8 and 10.3 ky B.P., and disappeared between 9.5 and 9.0 ky B.P. (*8*) (Fig. 5). Paleowetland deposits at Río Loa, Río Salado, and Quebrada Puripica, fed by strongly contrasting hydrologic systems, also record the mid-Holocene discharge increase seen at Tilomonte (*9*).

The combined data from middens and wetland deposits provide a detailed and replicated record of climatic change during the past 22 ky B.P. The paucity of both kinds of deposits for the period 35 to 16.2 ky B.P. suggests either selective preservation or greater aridity that decreased both local vegetation and rodent activity and regional snowpack and recharge in the Chilean Andes. Between 16.2 and 10.5 ky B.P., and particularly between 11.8 and 10.5 ky B.P., lowering of species ranges by up to 1000 m suggests that annual precipitation increased to ~70 to 100 mm at our driest site (2600 m), which today receives ~20 mm, and to 100 to 150 mm between 3000 and 3200 m, which now gets ~50 to 70 mm. Southward displacement of northern species and preponderance of summer-flowering herbs and C_4 grasses show that the precipitation increase happened in summer. Wetland deposits at Tilomonte identify higher groundwater levels between 15.4 and 9.0 ky B.P., consistent with increased precipitation in the Chilean Andes, but are not specific about

the seasonality of precipitation or time of maximum recharge and discharge (Fig. 4). Greatly diminished grasses abundance and taxonomic richness suggest abrupt drying between 10.5 and 10.3 ky B.P. (Fig. 3), whereas Tilomonte stratigraphy indicates lowering of the water table to modern levels between 9 and 8 ky B.P. (Fig. 4). After 8.0 ky B.P., the water table gradually rose until 3.0 ky B.P. This is consistent with slightly more mesic midden floras between 7.0 and 3.0 ky. The periods 9 to 8 ky B.P and after 3.0 ky B.P. mark times when vegetation and groundwater tables approached modern levels, perhaps the driest episodes in the past 22 ky B.P.

Our well-dated record for the central Atacama differs in several respects from paleoclimatic reconstructions elsewhere in the central Andes. Such discrepancies are common in paleoclimatic records throughout the region and may arise from poor dating, differences in regional climatologies across the broad (0° to 24°S) areas under discussion, or ambiguities between precipitation and temperature effects on glacial and lake budgets. For the past 22 ky B.P., the main disagreement is in the timing of maximum wetness and aridity since the Last Glacial Maximum. On the Bolivian Altiplano, maximum wetness is inferred from integration of the present Poopó, Coipasa, and Uyuni basins into the Tauca Phase highstand (3760 m), forming a ~50,000 km^2 paleolake (*10, 11*). The chronology for the Tauca Phase, based on ^{14}C dates of lacustrine carbonates, shows that lake levels began rising at ~18.4 ky B.P., reaching the highest stand between 16.2 and 14.0 ky B.P. Lake levels dropped sometime after 13.9 ky B.P. (Ticaña Event), but a moderate-sized lake (Coipasa Event) apparently persisted until 9.5 ky B.P. (*11*) (Fig. 5). Problems with hard-water effects on ^{14}C dates and detrital contamination on U-series dates make the lake desiccation chronology uncertain. The relation between lake desiccation and deglaciation in the central Andes is poorly known. In the tropical Andes (0° to 15°S), rapid ice recession is documented by 12.8 ky B.P. (*12*), well before the period (11.8 to 10.5 ky B.P.) of maximum summer precipitation in the central Atacama.

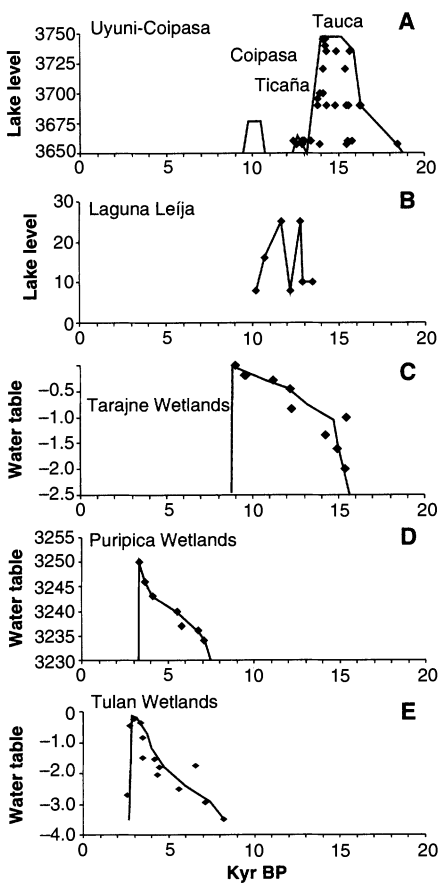

Fig. 5. Estimates (solid lines) of lake-level and water-table fluctuations reconstructed from calibrated ^{14}C ages or inferred ages (diamonds) from (**A**) Salares de Coipaso and Uyuni (*11*), (**B**) Laguna Lejia in the High Atacama (*7, 8*) and (**C** to **E**) wetland deposits from Quebrada Puripica (*9*) and our study sites.

A clear discrepancy with other regional records is our inference for a wet phase between 8 and 3 ky B.P., with groundwater discharge peaking between 5 and 3 ky B.P (Fig. 4). Although mid-Holocene middens contain mostly summer-flowering species, we acknowledge the possibility that greater winter snowpack in the High Andes could have raised regional groundwater levels without substantially increasing precipitation in the Prepuna–Absolute Desert transition. The mid-Holocene wet period in the central Atacama contrasts with the extreme lowstand of Lake Titicaca (15° to 17°S), 100 m below the present water level, between >6 and 3.8 ky B.P. (*13*), with high soluble and insoluble dust concentrations in the Sajama ice cores from 9000 to 3000 years ago (*14*), and with limnological evidence for drier conditions from Laguna Miscanti (*15*), just 30 km east of the Tilomonte spring complex (Fig. 2). Evidence for mid-Holocene aridity from Laguna Miscanti and other saline lakes on the Chilean Altiplano is uncertain because local ^{14}C reservoir effects require age corrections of several thousand years (*7, 8*). The Lake Titicaca lowstand, however, is well dated and corroborated among multiple lines of evidence in the immediate vicinity of the lake (*13*). One exception is a wet episode between 4.5 and 3.9 ky B.P. recorded by fluvial terraces and shallow lakes along the Rio Desaguadero, the only outlet to Lake Titicaca (*16*). This wet episode was not registered in the Lake Titicaca cores but is evident in a pollen stratigraphy from Laguna Seca (~18°S), 200 km south of Lake Titicaca and only 30 km southwest of Sajama (*17*). Resolution of these discrepancies may rest on better definition of response times and sensitivities to climatic events of varying duration and magnitude for vegetation, small and large lakes, and alluvial and groundwater systems.

Our well-dated chronologies from wetland deposits and rodent middens, specific to precipitation seasonality and amount, raise questions about what ultimately drives tropical rainfall variability on millennial time scales. Maximum summer precipitation (11.8 to 10.5 ky B.P.) in the central Atacama coincided with rapid regional warming (*14*) and rising global methane levels, thought to reflect expansion of tropical wetlands (*18*) during the Younger Dryas–Preboreal transition (11.8 to 10.5 ky B.P.) (Fig. 3). Paradoxically, wetter summers on the Pacific slope of the Andes happened during a time of minimum summer insolation at 20°S (*19*). Some authors have argued that this would have limited adiabatic heating over land and southward migration of the Intertropical Convergence Zone, reducing summer precipitation over southern Amazonia and the central Andes (*20*). This linear interpretation of seasonal (and regional) insolation, however, ignores atmospheric circulation anomalies over the central Andes that are linked to El Niño–Southern Oscillation. For example, westerly wind anomalies during El Niño events inhibit moisture advection from the east to the western part of the Bolivian Altiplano (and central Atacama), whereas strong easterlies during La Niña conditions favor convection and precipitation (*21*). Simulations with coupled ocean-atmosphere models suggest that El Niño intensity in the early Holocene was reduced by (i) strengthening of the Pacific trade winds by an intensified Asian monsoon due to increased summer insolation in the Northern Hemisphere (*22*) and (ii) a similar strengthening of the Pacific trade winds with differential cooling of the eastern relative to western Pacific by reduced summer insolation in the Southern Hemisphere (*23*). We conclude that the late glacial–early Holocene pluvial in the central Atacama Desert must have happened during a time of strengthened Pacific trade winds (easterlies) and persistent La Niña–like conditions.

References and Notes

1. T. P. Guilderson, R. G. Fairbanks, J. L. Rubensonte, *Science* **263**, 663 (1994); L. G. Thompson *et al.*, *Science* **269**, 46 (1995); M. Stute *et al.*, *Science* **269**, 379 (1995); P. Colinvaux, P. E. D. Oliveira, J. E. Moreno, M. C. Miller, M. B. Bush, *Science* **274**, 85 (1996).
2. The same methods for collecting and analyzing packrat middens in the southwestern United States were applied to rodent middens in the Atacama; J. L. Betancourt, T. R. Van Devender, P. S. Martin, Eds., *Packrat Middens: The Last 40,000 Years of Biotic Change* (Univ. of Arizona Press, Tucson, AZ, 1990).
3. The Atacama spring and wetland deposits have close analogs in the Great Basin, United States, where methods and approaches were developed and refined: J. Quade, M. D. Mifflin, W. L. Pratt, W. McCoy, *Geol. Soc. Am. Bull.* **107**, 213 (1995); J. Quade, R. M. Forester, W. L. Pratt, C. Carter, *Quat. Res.* **49**, 129 (1998).
4. Local and regional vegetation gradients are discussed in: C. Villagran, J. J. Armesto, M. T. K. Arroyo, *Vegetation* **48**, 3 (1981); C. Villagrán, M. T. K. Arroyo, C. Marticorena, *Rev. Chilena Hist. Nat.* **56**, 137 (1983); M. T. K. Arroyo, F. A. Squeo, J. J. Armesto, *Ann. Missouri Bot. Gard.* **75**, 55 (1988); C. Marticorena *et al.*, *Gayana Bot.* **55**, 23 (1998); P. A. Marquet *et al.*,

Rev. Chilena Hist. Nat. **71**, 593 (1998); M. T. K. Arroyo *et al.*, *Gayana Bot.* **55**, 93 (1999).

5. Ages are reported as calendar kiloyears B.P. All ^{14}C dates in the text and figures were converted to calendar ages with the program CALIB: v 4.0 (Intcal98) [M. Stuiver and P. J. Reimer, *Radiocarbon* **35**, 215 (1993)]. Grass abundance was measured as point occurrence on a 120-cell rectangular grid overlain on a sorting tray. A sediment matrix splitter was used to randomly segregate 100 ml of plant debris from each midden. Midden debris was spread uniformly across a 120-cell rectangular grid (each cell is 1 inch by 1 inch or ~6.45 cm^2); grass abundance was measured as point occurrence on the grid (the number of cells out of 120 where grass blades, florets, or seeds were identified). All plant remains were identified to the highest taxonomic level possible with a reference collection gleaned from herbarium specimens and our own field studies. In general, we met comparable success as with identifications of plant macrofossils in North American packrat middens.
6. Vascular plant remains, visible as carbonized wood, twigs, and leaves, are abundant in the wetland deposits. Other organic-rich samples are too fine grained or decomposed to identify the source and could suffer from hard-water effects on ^{14}C dates if partly algal in origin. Groundwater from springs in the Atacama displays hard-water or reservoir effects, typically containing $\leq 26\,^{14}C$ % modern carbon [R. Aravena and D. Suzuki, *Water Resources Res.* **26**, 2887 (1990)]. Evidence against a hard-water effect includes excellent stratigraphic coherence between dates from carbonized wood and other fine-grained organic matter and a date of 105 ^{14}C years B.P. on humates from a modern black mat.
7. M. Grosjean, *Palaeogeogr. Palaeoclimatol. Palaeoecol.* **109**, 89 (1994); M. Grosjean, M. A. Geyh, B. Messerli, U. Schotterer, *J. Paleolimnol.* **14**, 241 (1995).
8. M. Geyh *et al.*, *Quat. Res.* **52**, 143 (1999).
9. Extensive paleowetland deposits dating to the mid-Holocene are present on both the Rio Salado and Rio Loa, located 150 km north-northwest of Tilomonte. Mid-Holocene wetland deposits crop out 5 to 7 m above the modern wetlands. At the Rio Loa, the base of these deposits is not exposed, whereas samples from the middle and top of the section yielded ages of 4.9 and 3.5 ky B.P. Upper portions of the mid-Holocene wetland deposits at Rio Salado yielded ages between 6.7 and 4.3 ky B.P. Wetland deposits at Quebrada Puripica, dating between 7.1 and 4.4 ky B.P., were initially interpreted as paleowetland deposits formed from side-canyon damming by debris flows [M. Grosjean, L. Nuñez, I. Cartajena, B. Messerli, *Quat. Res.* **48**, 239 (1997)]. We found that the wetland deposits at Puripica were not debris-flow dammed but instead are similar to the deposits at Tilomonte and formed as a result of higher groundwater levels during the mid-Holocene.
10. M. Servant and J. C. Fontes, *Cah. ORSTOM Ser. Geol.* **10**, 5 (1978); B. Rondeau, thesis, Université du Québec à Montréal (1990); C. Clapperton, *Palaeogeogr. Palaeoclimatol. Palaeoecol.* **101**, 189 (1993); B. G. Bills *et al.*, *Geophys. Res. Lett.* **21**, 293 (1994); T. A. Blodgett, J. D. Lenters, B. L. Isacks, *Earth Interactions* **1** (1997) (http://ams.allenpress.com/amsonline/?request-get-archive&issn-1087-3562).
11. F. Sylvestre *et al.*, *Quat. Res.* **51**, 54 (1999).
12. D. T. Rodbell and G. O. Seltzer, *Quat. Res.*, in press.
13. D. Wirrmann and L. Oliveira, *Palaeogeogr. Palaeoclimatol. Palaeoecol.* **59**, 315 (1987); D. Wirrmann and P. Mourguiart, *Quat. Res.* **43**, 344 (1997); M. B. Abbott, M. W. Binford, M. Brenner, K. R. Kelts, *Quat. Res.* **47**, 169 (1997); P. Mourguiart *et al.*, *Palaeogeogr. Palaeoclimatol. Palaeoecol.* **143**, 51 (1998); G. O. Seltzer, P. Baker, S. Cross, R. Dunbar, S. Fritz, *Geology* **26**, 167 (1998); S. L. Cross, P. A. Baker, G. O. Seltzer, S. Fritz, R. B. Dunbar, *Holocene* **10**, 21 (2000).
14. L. G. Thompson *et al.*, *Science* **282**, 1858 (1998).
15. B. L. Valero-Garces *et al.*, *J. Paleolimnol.* **16**, 1 (1996); A. Schwalb, S. J. Burns, K. Kelts, *Palaeogeogr. Palaeoclimatol. Palaeoecol.* **148**, 153 (1999).
16. P. C. Baucom and C. A. Rigsby, *J. Sediment. Res.* **69**, 597 (1999).
17. C. A. Baied and J. C. Wheeler, *Mountain Res. Dev.* **13**, 145 (1993).
18. J. Chappellaz *et al.*, *Nature* **345**, 127 (1990); J. Chappellaz *et al.*, *Nature* **366**, 443 (1993); T. Blunier *et al.*, *Nature* **374**, 46 (1995).
19. A. Berger and M. F. Loutre, *Quat. Sci. Rev.* **10**, 297 (1991).
20. L. Martin *et al.*, *Quat. Res.* **47**, 117 (1997); M. B. Abbott, G. O. Seltzer, K. Kelts, J. Southon, *Quat. Res.* **47**, 70 (1997); G. Seltzer, D. Rodbell, S. Burns, *Geology* **28**, 35 (2000).
21. J. D. Lenters and K. H. Cook, *Mon. Weather Rev.* **127**, 409 (1999); R. D. Garreaud, *Mon. Weather Rev.* **127**, 901 (1999); M. Vuille, *Int. J. Climatol.* **19**, 1579 (1999); M. Vuille, R. S. Bradley, F. Keiming, *J. Geophys. Res.* **105**, 12447 (2000).
22. Z. Liu *et al.*, *PAGES Newsl.* **2**, 16 (1999).
23. A. C. Clement, R. Seager, M. Cane, *Paleoceanography* **14**, 441 (1999); M. Cane and A. C. Clement, in *Mechanisms of Global Climate Change at Millennial Time Scales*, vol. 112 of *Geophysical Monograph Series*, P. U. Clark, R. S. Webb, L. D. Keigwin, Eds., (American Geophysical Union, Washington, DC, 1999), pp. 373–383.
24. E. J. Brook, T. Sowers, J. Orchado, *Science* **273**, 1087 (1996); J. P. Severinghaus, T. Sowers, E. J. Brook, R. B. Alley, M. L. Bender, *Nature* **391**, 141 (1998); J. P. Severinghaus and E. J. Brook, *Science* **286**, 930 (1999).
25. We thank P. Marquet and L. Nuñez for field logistics; M. Arroyo, C. Villagrán, K. Zamora, A. Maldonado, Z. Naiman, C. Placzek, B. Saavedra, and H. Samaniego for field assistance; G. Cisneros, B. Gillis, and C. Holmgren for laboratory assistance; O. Matthei for grass identifications; J. Dohrenwend for map support; Geochronology Laboratory for conventional ^{14}C dates and the University of Arizona Accelerator Facility for accelerator mass spectrometry ^{14}C dates; J. Severinghaus for GISP2 methane data; L. Thompson for $\delta^{18}O$ and dust data from Sajama; and J. Cole, S. Jackson, M. Vuille, M. Cane, and A. Clement for discussions. This work was supported by an InterAmerican Institute grant to J.L.B. and V. Markgraf, National Geographic Society and NSF grants to J.Q. and J.L.B., and the U.S. Geological Survey. C.L. is supported by Comisión Nacional de Investigación Científica y Tecnología, Chile, with travel to Arizona provided by a U.S. Agency for International Development grant to B. Timmerman. J.A.R. is supported by a NASA grant.

12 May 2000; accepted 29 June 2000

Structural Evidence for Evolution of the β/α Barrel Scaffold by Gene Duplication and Fusion

Dietmar Lang,[1] Ralf Thoma,[2] Martina Henn-Sax,[3] Reinhard Sterner,[2,3,4] Matthias Wilmanns[1]*

The atomic structures of two proteins in the histidine biosynthesis pathway consist of β/α barrels with a twofold repeat pattern. It is likely that these proteins evolved by twofold gene duplication and gene fusion from a common half-barrel ancestor. These ancestral domains are not visible as independent domains in the extant proteins but can be inferred from a combination of sequence and structural analysis. The detection of subdomain structures may be useful in efforts to search genome sequences for functionally and structurally related proteins.

Enzymes from metabolic pathways are among the best-studied examples of protein function and structure. There are catabolic pathways, like glycolysis, or anabolic pathways, like tryptophan biosynthesis, where an almost complete database of protein structures is available. It is evident that many enzymes in these pathways have evolved either by gene duplication and fusion or by the assembly into functional oligomers (*1*, *2*). Molecular relations of proteins of the histidine and tryptophan biosynthesis pathways were postulated by structure prediction (*3*) and multisequence alignment methods (*4*). Many proteins in these pathways and other biological processes are folded as eightfold β/α barrels (*5*, *6*). Their evolution has been discussed (*7*, *8*) and has recently been mimicked in a directed evolution experiment (*9*). Here, we compare atomic structures of two enzymes in the histidine biosynthesis pathway and provide evidence for the evolution of β/α barrels from an ancestral half-barrel. The observation that ancestral folding units may comprise subdomain structural units has broad applications in searching genomic sequences for related gene products and their functional interactions in biological processes (*2*, *10*–*12*).

The crystal structures of the monomeric gene products HisA and HisF from the hyperthermophile *Thermotoga maritima* were deter-

[1]European Molecular Biology Laboratory (EMBL) Hamburg Outstation, EMBL c/o Deutsches Elektronen-Synchrotron (DESY), Notkestrasse 85, D-22603 Hamburg, Germany. [2]Abteilung für Biophysikalische Chemie, Biozentrum der Universität Basel, Klingelbergstrasse 70, CH-4056 Basel, Switzerland. [3]Abteilung für molekulare Genetik und Präparative Molekularbiologie, Institut für Mikrobiologie und Genetik, Georg-August-Universität Göttingen, Grisebachstrasse 8, D-37077 Göttingen, Germany. [4]Universität zu Köln, Institut für Biochemie, Otto-Fischer-Strasse 12-14, D-50674 Köln, Germany.

*To whom correspondence should be addressed. E-mail: wilmanns@embl-hamburg.de